



## Treatment of an *in situ* oil sands produced water by polymeric membranes

Mahsa Hayatbakhsh<sup>a</sup>, Mohtada Sadrzadeh<sup>a,\*</sup>, David Pernitsky<sup>b</sup>, Subir Bhattacharjee<sup>c</sup>, Javad Hajinasiri<sup>a</sup>

<sup>a</sup>Department of Mechanical Engineering, University of Alberta, 6-074 NINT Building, Edmonton, Canada AB T6G 2G8, Tel. +1 403 874 5038; email: [mahsa.hayatbakhsh@gmail.com](mailto:mahsa.hayatbakhsh@gmail.com) (M. Hayatbakhsh), Tel. +1 780 492 9099; Fax: +1 780 492 2200; email: [sadrzade@ualberta.ca](mailto:sadrzade@ualberta.ca) (M. Sadrzadeh), Tel. +1 780 604 7118; email: [hajinasi@ualberta.ca](mailto:hajinasi@ualberta.ca) (J. Hajinasiri)

<sup>b</sup>Suncor Energy Inc., P.O. Box 2844, 150-6th Ave. SW, Calgary, Canada AB T2P 3E3, Tel. +1 406 296 5119; email: [dpernitsky@suncor.com](mailto:dpernitsky@suncor.com)

<sup>c</sup>Water Planet Engineering, 721 S Glasgow Ave., Los Angeles, CA 90301, United States, Tel. +1 424 331 7700; email: [subir@waterplanet.com](mailto:subir@waterplanet.com)

Received 5 October 2014; Accepted 27 June 2015

---

### ABSTRACT

Cross-flow ultrafiltration (UF), nanofiltration (NF), and reverse osmosis (RO) were applied for the first time on a produced water obtained from a thermal *in situ* bitumen recovery process called steam-assisted gravity drainage (SAGD), with the intent to remove salt, silica, and dissolved organic matter (DOM) so that the produced water could be re-used as high-quality boiler feedwater. It was found that more hydrophilic and more negatively charged membranes were less susceptible to fouling. The UF membrane tested rejected a maximum of 30% of the salt and silica and 50% of the DOM. Nanofiltration with loose membranes removed more than 70% of the salt and DOM. The tight NF membranes tested removed more than 86% of the salt, silica, and DOM, and consumed less energy than RO, which showed almost the same rejection. An instantaneous increase in water flux resulting from a step change in feedwater pH demonstrated the critical role of pH in flux recovery and in fouling mitigation. Analysis of the fouled membranes indicated presence of silica, iron, and calcium in the foulant material. Feed and permeate characterization showed that mainly hydrophilic DOM passed through the membrane. The study provides valuable insights regarding the suitability of membranes as alternatives to conventional SAGD water treatment methods, especially in terms of producing higher quality recycled water.

**Keywords:** Oil sands; SAGD; Membrane processes; Produced water treatment; Reverse osmosis; Nanofiltration; Ultrafiltration

---

### 1. Introduction

Steam-assisted gravity drainage (SAGD) is a thermally enhanced heavy oil recovery method which is widely practiced for bitumen extraction from oil sands

in Alberta, Canada. In this process, steam is injected through a horizontal well into the bitumen-containing formation to decrease the viscosity of the bitumen and effect its extraction. An emulsion of steam condensate and heated bitumen flows down along the periphery of the steam chamber to the production well which is located below the injection well. This emulsion is then

---

\*Corresponding author.

pumped to the surface where the bitumen and water are separated and the water is treated for reuse as boiler feedwater (BFW).

In a typical SAGD surface treatment plant, the produced emulsion is first sent through a series of gravity separation vessels to remove the gases, and separate the bitumen and water. The produced water is then deoiled utilizing oil skimmers, as well as induced gas flotation devices. Finally, the water passes through an oil removal filter to remove traces of free oil and grease from the water. In a conventional SAGD water treatment plant, the de-oiled produced water mixes with make-up water and recycled boiler blow-down (BBD) water to make the inlet stream for a warm lime softener (WLS). This stream, called WLS inlet water, is at pH 9–10 and its silica, total organic carbon (TOC), and total dissolved solid (TDS) concentration is in the range of 50–100, 300–500, and 1,500–2,000 mg/L, respectively. About 90% of the silica is removed by warm lime softening and a media filter is used to remove the residual particles. In order to further remove dissolved divalent ions like  $\text{Ca}^{2+}$  and  $\text{Mg}^{2+}$  to make the treated water suitable for BFW, a weak acid cation exchanger (IX) is used downstream of the WLS. The treated water is used as BFW for a robust style of steam generator known as a once through steam generator (OTSG), which can tolerate relatively high amounts of TDS and TOC. To compensate for the relatively low-quality BFW, however, OTSGs typically produce only a low quality steam (75–80%), resulting in a large volume of boiler blowdown (BBD). A portion of the BBD is recycled back to the WLS and the rest is sent to disposal.

The economics of an SAGD process depend on the energy consumed for steam generation as well as the energy consumed for produced water deoiling and treatment and blowdown disposal [1,2].

The conventional WLS-IX water treatment configuration does not reduce the amount of dissolved organic matter (DOM) or salinity (TDS) in the BFW. The high levels of DOM and TDS in the OTSG feedwater can cause numerous operational problems like fouling of pipelines and equipment, and clogging of injection wells [2–4]. To reduce the injection water volume, evaporators are sometimes used as a downstream BBD recovery process. Evaporators have also been used to directly desalinate produced water to make high-quality BFW, but energy use is high. High boiler feedwater TDS and DOM results in higher blowdown volumes and necessitates recycling more low quality BBD water back to the process [4]. The chemical intensive WLS-IX scheme also suffers from high operating cost, large foot print, and excessive recycles. The major chemicals added in the WLS are

lime and magnesium oxide. The IX system requires polymeric resins and regenerations chemicals. Other chemicals in the form of coagulants and polymers are also required, which increases the operating cost of the current process [5]. In light of the above, it is of interest to compare the WLS-IX scheme with an alternative membrane-based process which can separate almost all silica and divalent ions and reject more than 90% of DOM and TDS in a single step operation [6]. In addition to improving operation of the current OTSGs, a membrane-based desalination process would allow the production of high-quality BFW suitable for higher efficiency drum boilers, while consuming less energy than if desalination evaporators were used.

Among emerging technologies applied for oilfield produced water treatment [7], membrane separation processes have been found to be attractive candidates due to their lower operating expenses and lower energy consumption. Although microfiltration (MF) and conventional ultrafiltration (UF) membranes have been shown to be ineffective for the separation of silica, DOM and salt from produced water [8–10], tighter UF membranes have been reported to remove up to ~60% of the organic matter and silica, depending on the characteristics of feedwater constituents and the operating conditions (pH and ionic strength), while consuming relatively low amounts of energy [8,11,12]. Nanofiltration (NF) and reverse osmosis (RO) are widely used for separation of organic matter, salt, and silica from water and wastewater. However, there are few records in the peer-reviewed literature for their application in desalination and organic removal from oil sands produced water [13–16]. This is mainly due to their high susceptibility to fouling by the high TDS and high TOC concentrations in SAGD produced water, and the unfamiliarity of the SAGD industry with water treatment membrane technology.

Fouling is the principal obstacle in developing a sustainable and energy efficient membrane process for SAGD applications. It significantly reduces membrane performance and membrane lifetime, and subsequently increases operation and maintenance costs [17]. The extent of membrane fouling by DOM is, of course, related to the concentration and nature of the DOM in the membrane feedwater. SAGD-produced waters are known to have high DOM concentrations, so organic fouling is anticipated to be significant. The characteristics of the DOM present in SAGD produced waters are only beginning to be characterized in detail. Peng et al. [14] and Kim et al. [13] studied membrane fouling by oil sands process affected water (OSPW) associated with the surface extraction of bitumen; OSPW primarily contains naphthenic acid-like DOM [18–22]. Kawaguchi et al. [23] showed that

naphthenic acids also predominated in SAGD process water samples (>74% of the organic acids), while traces of fatty acids (originating from the groundwater used as makeup water) were also found. They indicated that the nature of the DOM in the SAGD-produced water changed through the water treatment process. Petersen and Grade [24] divided organic species in SAGD-produced water samples into three primary groups: saturated aliphatics (*n*-alkane and cycloalkane), aromatics (benzenes and polyaromatic rings), and polar compounds (alcohols, ketones, phenols, etc.), all indicative of the presence of naphthenic acids as the main DOM group in SAGD-produced water. However, Guha Thakurta et al. [4] found that the DOM found in SAGD-produced waters are significantly different from OSPW DOM, and more like humic acids than naphthenic acids. It must be noted that every DOM molecule has a specific charge and molecular conformation which controls the rate of fouling and subsequently the performance of the membrane process [25]. Also, the interaction of DOM functional groups with other ions in solution (such as silica), and changes in the DOM functional groups with solution pH alter the properties of the DOM and subsequently influence the structure and hydraulic resistance of the fouling layer on the membrane [17,26–28].

Few reports of membranes being tested for SAGD-produced water treatment are found in the open literature. The aim of this study, therefore, was to investigate the performance of commercial UF, NF, and RO membranes for desalination, hardness, silica, and DOM removal from SAGD produced water samples obtained from operating facilities in the Athabasca oil sands region. The effects of membrane hydrophilicity, zeta potential, roughness, and pore size on flux decline and TOC and TDS rejection were investigated using a bench-scale, flat-sheet membrane testing apparatus.

## 2. Material and methods

### 2.1. Feedwater

SAGD WLS inlet water was obtained from an SAGD water treatment plant located in the Athabasca oil sands region of Alberta, Canada and shipped to the University of Alberta for testing. Samples were collected in sealed containers and kept under a nitrogen blanket until they were opened for the treatment experiments. The pH, conductivity, and TOC of the samples were measured (Table 1). The concentration of dissolved silica and other inorganic ions was measured by inductively coupled plasma-optical emission

Table 1  
Properties of WLS inlet water

Elements	Units	Feed water
pH	–	9
Conductivity	μS/cm	1,680
TDS	mg/L	1,200
TOC	mg/L	420
Dissolved silicon (Si)	mg/L	89
Sodium (Na <sup>+</sup> )	mg/L	350
Chloride (Cl <sup>-</sup> )	mg/L	170
Calcium (Ca <sup>2+</sup> )	mg/L	1.9
Magnesium (Mg <sup>2+</sup> )	mg/L	0.59
Iron (total Fe)	mg/L	0.39
Boron (B)	mg/L	19

spectrometry (ICP-OES). The chloride concentration was measured by automated colourimetry using the SSMA 4500 CL-E method. TDSs was measured using the SM 2540-C protocol. The data presented in Table 1 indicates that the WLS inlet water contained high concentration of DOM, TDS, and dissolved silica, as expected.

### 2.2. Membranes

Membrane filtration experiments were conducted using six types of polymeric membranes: three NF membranes (NF270 and NF90 from Filmtec and ESNA from Hydranautics), two RO membranes (BW30 from Filmtec and ESPA from Hydranautics), and one UF membrane (thin film UF from GE). All of these membranes are thin film composite membranes consisting of three layers: a thin film as an active layer, an intermediate microporous layer, and a mesoporous polyester fabric support [29]. The very thin polyamide (PA) active layer determines the membrane separation properties and fouling behavior.

The properties of the membranes were obtained from the manufacturers' product manuals and literature, and are summarized in Table 2. As can be seen, all of the membranes tested can withstand feed temperatures and pH as high as 45°C and 10, respectively. The main characteristics which govern the permeation properties of the membranes are the membrane molecular weight cut-off (MWCO), surface charge, hydrophilicity, and roughness. MWCO is defined as the molecular weight for which 90% of a test solute, usually polyethylene glycol (PEG), is retained by the membrane [30]. The higher the MWCO, the larger the pore size of the membrane. Membranes having higher MWCO, for example the UF membrane used in this

Table 2  
Properties of tested polymeric membranes

Membrane properties	NF270 (Filmtec)	NF90 (Filmtec)	BW30FR (Filmtec)	UF TF (GE)	ESNA (Hydranautics)	ESPA (Hydranautics)
Membrane type	NF polyamide thin-film composite	NF polyamide thin-film composite	RO polyamide thin-film composite	UF polyamide thin-film composite	NF polyamide thin-film composite	RO polyamide thin-film composite
Maximum operation pressure (kPa)	4,136	4,136	4,136	2,758	4,136	4,136
Maximum operation temperature (°C)	45	45	45	50	45	45
pH range, continuous operation	2–11	2–11	2–11	1–11	2–10	2–10
Salt rejection (%)	40–60	85–95	99.5	N/A	75–92	99.3
MWCO (Da)	330 ± 48 [31–33]	201 ± 25 [31–33]	116 ± 30 [31,34]	3,000	223 ± 37 [35,36]	125 ± 35 [34,37]
Contact angle ( $\theta^\circ$ )	34 ± 5.5 [31,38]	62 ± 6.7 [26,29,31]	63 ± 7.3 [29,31,38]	42 ± 3.4 [39,40]	60 ± 6.2 [35,36,41]	56 ± 6.0 [42,43]
Zeta potential (mV)	–12.1 at pH 4.5 [26,29] –21.6 at pH 7 [32] –24.0 at pH 9 [38]	5.1 at pH 4.5 [44] –24.9 at pH 7 [45] –27.3 at pH 9 [44]	–12.1 at pH 4.5 [29] –20.0 at pH 7 [38] –26.0 at pH 9 [38]	–21.8 at pH 7 [39] –28.8 at pH 8 [41]	0.0 at pH 4.5 –11.5 at pH 7 –11.0 at pH 9 [36,41]	–11.1 at pH 4.5 –26.0 at pH 7 [46] –26.8 at pH 9 [46]
Isoelectric point (IEP, KCl 10 <sup>–3</sup> M)	3 ± 0.20 [47,48]	4.0	4.0	N/A	4.9 ± 0.10 [47,48]	4.0 [46]
Mean roughness (nm)	5 ± 0.25 [25,38,49]	65 ± 2.2 [25,49,50]	65 ± 3.4 [29,38,49]	N/A	50 ± 3.5 [51,52]	73 ± 5.5 [37,42,46,51]

Note: Data were obtained from the membrane manufacturers' literature, unless otherwise indicated.

research, are more susceptible to fouling than denser membranes due to the higher permeation drag.

Bench-scale membrane experiments were conducted at a constant initial permeation flux so that permeation drag was constant for all membranes. This allowed fouling intensity to be compared to other surface properties like surface charge, hydrophilicity, and roughness. The surface charge and hydrophilicity of a membrane are quantified by measuring the zeta potential and contact angle. More negatively charged and more hydrophilic membranes are less prone to fouling by hydrophobic organic and negatively charged inorganic materials. Membrane surface roughness also plays a major role in fouling, until the cake layer grows thick enough to make the initial surface roughness less significant. Rougher surfaces favor the entrapment of foulants in the eddy zones occurring behind the peaks. Clogging of valleys on the surface of salt-rejecting NF and RO membranes results in significant loss of permeate flux [53].

### 2.3. Cross-flow membrane filtration setup

A schematic view of the cross flow membrane filtration setup used in this work is shown in Fig. 1. The setup consisted of a stainless steel feed tank, a membrane cell, a constant flow diaphragm pump of maximum capacity 6.8 LPM (1.8 GPM) from Hydra-Cell, a chiller/heater (Isotemp 3013, Fisher Scientific) to keep the feed temperature at 50°C, a bypass valve, and a back pressure regulator to control applied pressure and cross flow velocities (Swagelok). A digital weighing balance (Mettler Toledo) was used to measure the permeate flow rate and the data were directly collected into a computer using LabVIEW (National Instruments) data acquisition software.

### 2.4. Experimental methodology

Six experiments were conducted to find the effects of pH and membrane properties on water flux, TOC, and TDS rejection, and the deposition of organic and

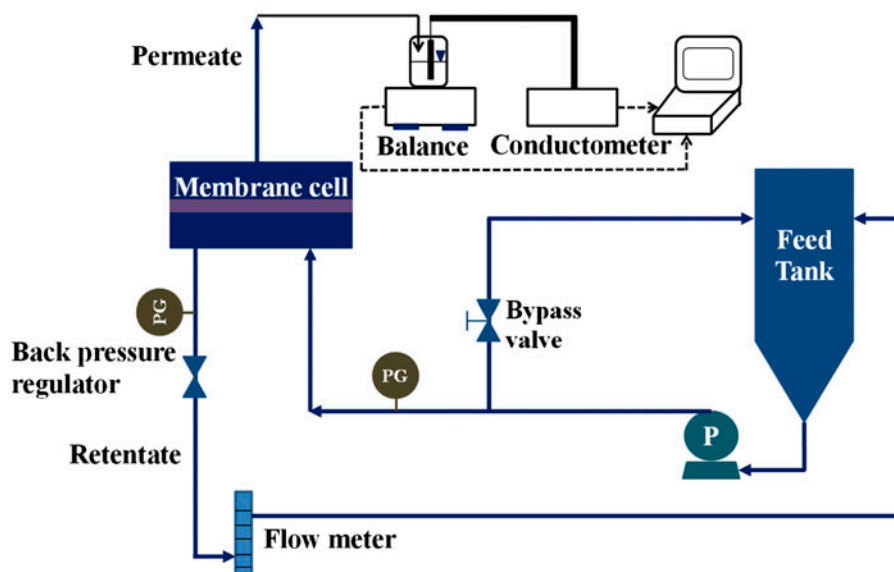


Fig. 1. Schematic view of cross-flow filtration setup.

inorganic matter on the membrane surface (Table 3). Constant pH (raw WLS inlet water pH 9) experiments were conducted on the NF270, ESNA, and ESPA membranes, and dynamic pH experiments (9–7–10) were carried out on the UF-TF, NF90, and BW30 membranes. Membrane samples were stored in de-ionized water for 24 h in order to remove preservatives. Before each experiment, membrane compaction was performed with de-ionized water at a pressure range of 800–1,400 kPa, depending on the type of membrane.

## 2.5. Characterization techniques

### 2.5.1. Fluorescence excitation emission matrix spectroscopy (FEEMs)

Fluorescence excitation–emission matrix spectroscopy (FEEMs) was used to analyze the fingerprint

of soluble and insoluble organic matter in water samples. A wavelength range of 200–500 nm with 5 and 10 nm intervals for excitation and emission wavelengths, respectively, was used. The WLS inlet samples were diluted using DI water to a TOC level of approximately 15 mg/L to avoid inner filtration (quenching) effects on the fluorescence analysis. For all experiments, fluorescence analysis was performed on feed and permeate samples at pH 9.

### 2.5.2. Total organic carbon (TOC)

The TOC measurement detects the concentration of all organic carbon atoms covalently bonded in the organic molecules of a sample of water. It is a parameter for monitoring the amount of DOM present in a sample, and for evaluating the efficiency of the water treatment process for organics removal. TOC is calculated based on total carbon (TC) and inorganic carbon (IC) measurements ( $TC - IC = TOC$ ). TOC in the present work was measured using a TOC analyzer (Shimadzu, model TOC-V; detection range 3–25,000 mg/L). All samples were filtered with 0.22  $\mu\text{m}$  MF membranes (Cellulose Acetate, Millipore, USA) to remove the suspended solids before TOC analysis.

### 2.5.3. Inductively coupled plasma-optical emission spectroscopy (ICP-OES)

Emission spectroscopy using ICP is a rapid, sensitive, and convenient method for the determination of metal ions in aqueous solutions. The concentration of

Table 3  
Variation of pH with time in conducted experiments

Membrane	Time (h)		
	1–2	3–4	5–6
UF-TF (GE)	pH 9	pH 7	pH 10
NF90 (Filmtec)	pH 9	pH 7	pH 10
BW30 (Filmtec)	pH 9	pH 7	pH 10
NF270 (Filmtec)	pH 9	pH 9	pH 9
ESPA (Hydranautics)	pH 9	pH 9	pH 9
ESNA (Hydranautics)	pH 9	pH 9	pH 9

dissolved silica and other inorganics presented in Table 2 was measured by an ICP-AES instrument (Agilent 735 ICP-OES) using EPA Method 200.7. In this method, the water sample is nebulized and the resulting aerosol is transported into an inductively coupled argon plasma generated by radio frequency power. The high temperature (6,000–10,000 K) of the plasma leads to almost complete dissociation of molecules and efficient atomization and ionization in the sample. Emission spectra are produced when the excited atoms and ions return to lower energy states. The spectra are dispersed by a high resolution echelle polychromator and the intensities of the lines are monitored by a charged coupled device. In OES, the power of the radiation emitted by a constituent after excitation is directly proportional to its concentration.

#### 2.5.4. Field-emission scanning electron microscope–energy dispersive X-ray (FESEM–EDX) analysis

A FESEM was used to provide images of the membrane surface to analyze surface morphology. Prior to the analysis, the membranes were coated with a thin film of chromium. Surface images of the membranes were obtained by using a JEOL 6301F FESEM. All membranes were imaged at a magnification of 20,000 times. FESEM was used to provide qualitative information on the deposition of foulants on the membrane. Semi-quantitative elemental analysis was also done, using a PGT IMIX energy dispersive X-ray (EDX) system with 135 eV resolution.

#### 2.5.5. Attenuated total reflectance-Fourier transform infrared (ATR-FTIR) spectroscopy

ATR-FTIR spectroscopy was used to provide information on the type of functional groups present on the membrane surface at depths of less than 1  $\mu\text{m}$  below the surface. Membranes were analyzed with ATR-FTIR before and after filtration with a Thermo Nicolet Nexus 670 FTIR instrument. This instrument is equipped with a mercury–cadmium–tellurium (MCT) detector and has a resolution of 4  $\text{cm}^{-1}$ . A total of 512 scans were averaged for each spectral measurement. The internal reflection element was a zinc selenide (ZnSe) ATR plate with an aperture angle of 45°. All membrane samples were scanned over the range of 600–4,000  $\text{cm}^{-1}$ .

### 3. Results and discussion

Membrane performance was evaluated on the basis of the permeation flux and the rejection of the target

contaminants. The fouling tendency of the membranes tested and the fouling potential of the water being treated were evaluated by measuring the rate of water flux decline over time. Fouling deteriorates the performance of membranes by decreasing the permeation flux and decreasing membrane life [25]. Membrane fouling is influenced by a great number of parameters including hydrodynamics (feed flow rate, permeation drag, and feed channel dimensions), solution chemistry (salt and divalent ion concentrations, the presence of sparingly soluble solids, and pH), and the surface properties of the membrane (hydrophilicity/hydrophobicity, zeta potential, surface roughness, and pore size). Regardless of the feedwater properties and the membrane module hydrodynamics, membrane manufacturers are continuously seeking to develop antifouling membranes by modifying their surface properties. In the present work, the effects of hydrophilicity, surface charge, and roughness of various types of polymeric membranes on the water flux and TOC and TDS rejection during UF, NF, and RO of SAGD produced water were investigated. Experiments were conducted at a constant feed flow rate and a constant permeation flux on the same industrial water sample (WLS inlet water), to minimize the effects of feed chemistry and hydrodynamics. Despite the many modification and fouling preventive strategies, membrane fouling is inevitable. Online reduction of membrane fouling by physical techniques like vibration, ultrasound, vortex generation, and flow and pressure pulsation have been widely studied [54–56]. Another technique for mitigating fouling during operation is the rapid change of operating conditions such as solution pH, ionic strength, and temperature, as well as the presence of light and electric and magnetic fields [57–59]. In this study, the effect of rapid changes in solution pH on water flux and TOC and TDS rejection was investigated. Since membrane filtration performance is known to be influenced by the characteristics of the feedwater and the interaction of its constituents with the membrane surface, the feed water, permeate, and the surfaces of the fouled membranes were characterized in detail.

#### 3.1. Continuous operation at fixed pH

Water flux and TOC/TDS rejection for the NF270, ESNA, and ESPA membranes at 50°C and a constant pH of 9.0 are shown in Fig. 2. An initial water flux of 35 LMH was used for all membranes, and was obtained by adjusting the feed pressure to 276, 552, and 827 kPa for the NF270, ESNA, and ESPA membranes, respectively. As can be observed in Fig. 2, water flux declined due to the combined fouling of

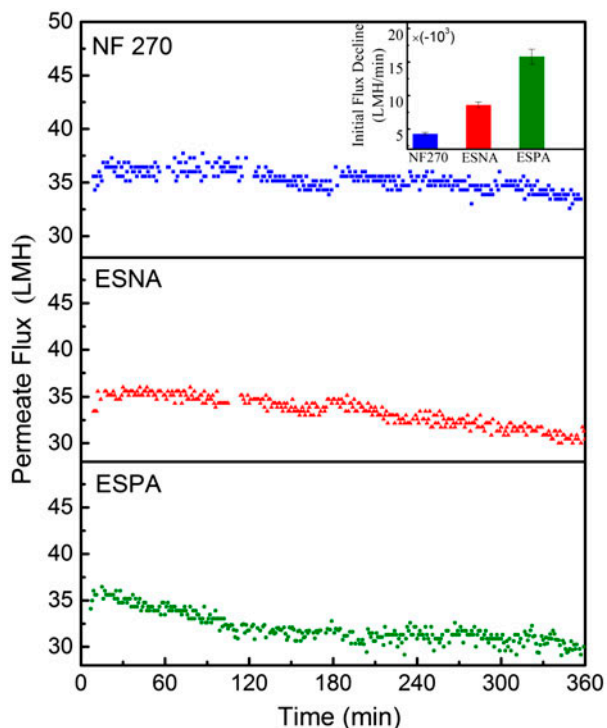


Fig. 2. Water flux decline during cross-flow filtration of WLS inlet water by NF270, ESNA, and ESPA membranes at constant pH 9. The transmembrane pressure was adjusted to 276, 552, and 827 kPa for NF270, ESNA, and ESPA membranes, respectively.

silica, organic matter, and divalent ions present in the WLS inlet water. According to Table 1, the concentration of silica and divalent ions in the WLS inlet water (~90 mg/L) is almost five times lower than the concentration of organic matter (420 mg/L). Hence, DOM fouling is expected to be the principal fouling mechanism in the present work. The initial adsorption of DOM onto the membrane surface decreases the permeate flux due to DOM gel formation, pore blocking, and induced hydrophobic properties.

Flux decline due to pore blocking and pore constriction was found to be more severe with membranes having a larger pore size (UF and loose NF membranes). For salt-rejecting NF and RO membranes, the plugging of hot spots by DOM was thought to be responsible for the sharp initial flux decline [38,53,60–62]. Hot spots are the valleys on the membrane surface with the minimum thickness and the maximum local water flux. Rapid clogging of these hot spots leads to substantial loss of permeate flux [53]. It has also been reported that the hydrophobicity of hydrophilic membranes increases after fouling by highly hydrophobic organic matter [38,63]. Increasing hydrophobicity generally leads to more susceptibility

to fouling due to the hydrophobic interactions between the membrane surface and the hydrophobic materials [38]. In this study, the organic matter present in the WLS inlet feedwater has been reported to be mainly hydrophobic acids (humic type) [4]. Since all of the membranes tested were hydrophilic (based on the contact angle values in Table 1), it was expected that the membrane surfaces would become hydrophobic after fouling.

The bar chart in Fig. 2 shows that the initial flux decline for the NF270 membrane was lower than the two other NF membranes. At the constant initial permeate flux, feed flow rate and feed solution chemistry (pH and ionic strength), the rate of flux decline was found to be strongly dependent on the surface properties of the membrane. According to the surface roughness and contact angle values presented in Table 2, the NF270 membrane is smoother and has stronger hydrophilic properties than the ESNA and ESPA membranes. In addition, the surface of the NF270 membrane is more negatively charged than that of the ESNA membrane. Earlier studies found that membrane surfaces with more negative zeta potentials and higher hydrophilicity exhibit less fouling by organic matter due to the higher electrostatic repulsion and lower hydrophobic interaction between the foulant and the membrane surface [38,64]. The ESNA membrane showed less initial decline than the ESPA membrane, in spite of being less negatively charged. The rougher surface of the ESPA membrane results in enhanced deposition of silica particles onto the membrane surface and, hence, more severe fouling [65], as it is expected that colloidal fouling governs in combined organic/colloidal fouling for rougher membranes. Meanwhile, the higher salt rejection seen with the ESPA membrane during these fouling experiments resulted in a more severe osmotic pressure build-up near the membrane surface and hence a greater flux decline [66].

It is worth noting that all membranes were tested at a permeation flux of 35 LMH, which is hypothesized to be close to their limiting flux, according to the moderate flux decline (7–10%) seen after the 6 h experiment. A higher initial permeation flux could have resulted in a more severe flux decline. Tu et al. [38] observed 50 and 30% water flux declines after 6 h of filtration of a humic acid and silica solution by an NF270 membrane at an initial permeate flux of 85 LMH. The NF270 membrane had a higher flux decline than a BW30 membrane tested under the same conditions. The higher flux decline of the NF270 membrane was attributed to the governing effect of the initial permeation flux, despite the NF270 membrane having lower surface roughness and higher negative

zeta potential and hydrophilicity than the BW30 membrane.

In earlier studies, membrane fouling has been described as involving two successive stages, where foulant–membrane and foulant–foulant interactions govern the deposition of material at the first and second stages, respectively [67–69]. Very low values of initial permeate flux decline in the NF270, ESPA, and ESNA membranes implies that foulant–membrane interaction is minimized either by the favorable surface properties of membranes tested or the hydrodynamic conditions of the experiments. When there is significant interaction between the foulant and the membrane, foulants (mainly DOM in the present work) will adsorb onto the membrane surface and decrease the permeate flux sharply, due to pore blocking, induced hydrophobic properties, and lowered permeation drag [27,38,70,71].

Fig. 3 shows the variation of TOC and TDS rejection with time using the NF270, ESPA, and ESNA membranes. As can be observed for all of these membranes, TOC rejection increased with time, which is evidence of hydrophobic interactions in the second

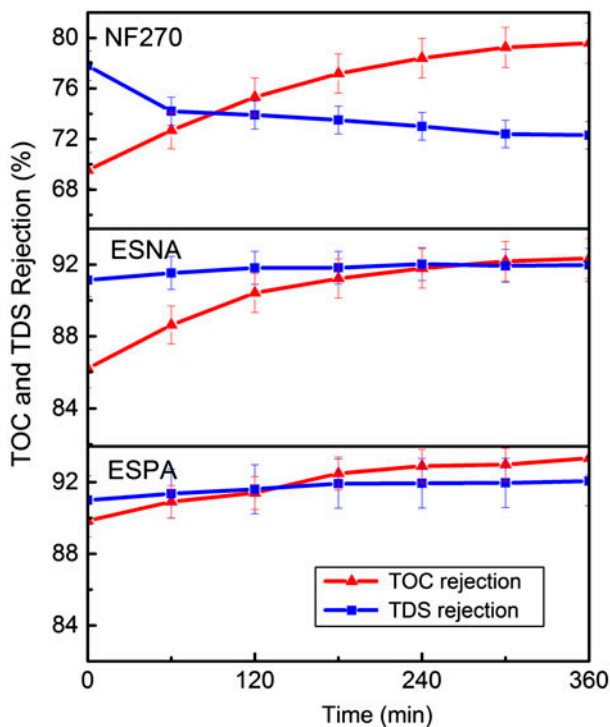


Fig. 3. TOC and TDS rejection during cross-flow filtration of WLS inlet water by NF270, ESNA, and ESPA membranes at constant pH 9. The transmembrane pressure was adjusted to 276, 552 and 827 kPa for NF270, ESNA, and ESPA membranes, respectively.

stage of fouling. According to the literature, the adsorption of organic matter on the membrane surface makes the membrane more hydrophobic [27,38,71,72]. This intensifies the deposition of new organic matter on previously deposited organic matter due to hydrophobic foulant–foulant interactions. As a result, TOC rejection increases. For the more hydrophilic NF270 membrane, the rate of increase in TOC rejection was greater. This result can be explained by the findings of Cho et al. [63] and Tu et al. [38], who both observed more severe induced hydrophobicity for more hydrophilic membranes after fouling by organic matter.

TDSs rejection remained constant for the more salt rejecting ESPA and ESNA membranes (>90% rejection), whereas TDS rejection decreased for the looser NF270 membrane. According to the literature, for salt rejecting membranes, both flux and salt rejection decline as fouling progresses due to cake enhanced concentration polarization [66,73]. As foulants (silica and organic matter) deposit on the membrane surface, the salt concentration at the membrane surface significantly increases because back diffusion of salt away from the membrane surface is hindered by the foulant cake layer [74]. The increased salt concentration at the membrane surface increases the driving force for salt transport through the membrane. This results in a significant passage of salt to the permeate stream and consequently a decrease in the TDS rejection. However, in this study, TDS rejection increased slightly for the denser membranes, which confirms the dominance of organic fouling for WLS inlet water filtration. The plugging of hot spots by organic matter is thought to have resulted in the formation of a denser screening layer which restricted the transport of salt, in agreement with previous findings reported in the literature [38,53,60–62].

For the NF270 membrane, however, TDS rejection decreased, which was not expected based on the lower fouling potential of this membrane, as discussed above. Lee et al. [74] showed that there is not necessarily a direct relationship between the rate of flux decline (fouling severity) and rejection decrease. They observed a much greater salt rejection drop for an NF membrane compared to a RO membrane, despite both membranes having similar flux decline trends. They attributed this to different mechanisms governing salt rejection for NF and RO. The predominant mechanism of salt rejection for RO membranes is size exclusion, while for NF membranes both size and charge (Donnan) exclusion are critical. Hence, a salt concentration increase on the membrane surface due to cake formation has a more significant effect for the charge exclusion mechanism.

### 3.2. Membrane operation with varying pH

Dynamic pH experiments were conducted on the UF, NF90, and BW30 membranes. The transmembrane pressure was adjusted to 207, 552, and 827 kPa, respectively, to achieve the same initial permeation flux of 35 LMH for all membranes. To determine the effect of pH on membrane performance, the pH of the WLS inlet feed was decreased rapidly from 9 (raw WLS inlet feed pH) to 7 after 120 min, then rapidly increased to 10 after 240 min. The variation of water flux with time and pH is shown in Fig. 4. Decreasing the pH from 9 to 7 resulted in a sharp decline in water flux for all membranes. Flux increased by increasing the pH from 7 to 10. The sharp flux decline was found to be more severe in the salt rejecting NF90 and BW30 membranes. Flux recovery became more evident for the denser BW30 membrane. The FESEM images, as will be shown later, indicated re-dissolving of the fouled material on the NF and RO membranes by increasing pH, which resulted in reversible fouling and flux recovery. By increasing the pH from 7 to 10,

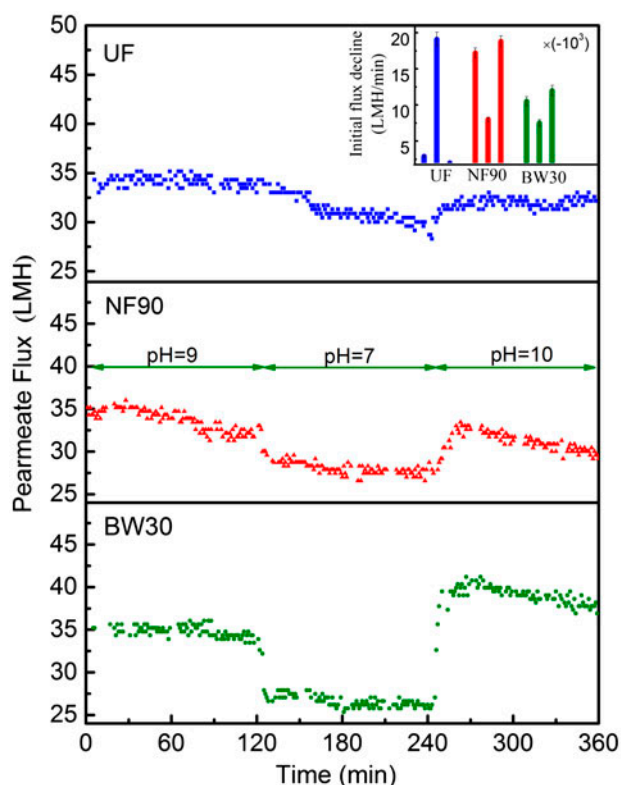


Fig. 4. Water flux decline during cross-flow filtration of WLS inlet water by UF, NF90 and BW30 membranes at various pH values (9–7–10). The transmembrane pressure was adjusted to 207, 552, and 827 kPa for UF, NF90 and BW30 membranes, respectively.

the flux increased to an even higher value than the initial flux at the initial raw WLS inlet water pH. Decreasing the pH increases the rate of co-precipitation of organic matter and silica, which causes a sharp flux decline, especially for denser membranes [4,75]. This is attributed to the quick change of foulant/foulant and foulant/membrane interactions by pH alteration.

The variation in permeate flux with pH change is due to changes in the properties of both the membrane and the solution. Silica and DOM are the major constituents in the WLS inlet water. The surface charge of silica particles is negative at pH values greater than their isoelectric point ( $\text{pH} > 3$ ). The magnitude of the silica surface charge increases with increasing pH and increasing salt concentration [76,77]. The surface charges of DOM functional groups are known to become more negative with increasing pH [17,78,79]. The higher negative charge on the DOM functional groups results in the formation of a more porous cake layer (due to the inter-foulant repulsion) and consequently results in higher permeation flux rates. The protonation of DOM functional groups (mainly COOH) at lower pH decreases the charge and ultimately the electrostatic repulsion [17,78–82]. Also, pH affects the macromolecular conformation of DOM, so that a smaller configuration occurs at lower pH values [17,27,83]. This causes the formation of a more compact fouling layer and subsequently, a flux decline, at lower pH values.

In addition to foulant/foulant interactions, foulant/membrane interactions strongly affect membrane performance at various pHs. Generally, the zeta potential of the membranes, particularly polyamide membranes containing carboxylic ( $\text{R-COO}^-$ ) and amine ( $\text{R-NH}_3^+$ ) ionizable functional groups, becomes more negative as pH increases [64,84]. Altogether, both inter-particle and particle-membrane repulsions prevent the particles from depositing, and lead to the formation of a thinner fouling layer. Hence, higher permeation fluxes were observed at higher pH values [17,27,28,50].

At the raw water pH, the minimum and maximum initial flux decline was observed for the UF and NF90 membranes, respectively (bar chart in Fig. 4). Based on the data presented in Table 2, the UF membrane is more hydrophilic and negatively charged than both the BW30 and NF90 membranes. This resulted in less flux decline at the constant permeation flux. Taking a closer look at Table 2, it is found that the BW30 and NF90 membranes have almost the same surface properties (roughness, contact angle, and zeta potential values) and are therefore predicted to show the same fouling behavior. The slightly higher fouling

seen with the NF90 membrane can be attributed to minor pore blocking by DOM with molecular weight less than 250 Da. Our previous study showed that almost 40% of the DOM in the BBD has a molecular weight less than 500 Da [4]. This small molecular size increases the chance of pore blocking by DOM in membranes having MWCO in the range of 100–300 Da (see Table 2). At pH 7, exactly the opposite behavior compared to pH 9 was observed. At lower pH, when co-precipitation of silica and organic matter occurs, the size of the deposited materials increases, which makes pore blocking more severe. FESEM images of fouled membranes showed the presence of particles with a diameter of 100 nm, as will be discussed later.

Fig. 5 shows the effect of a step change in pH on TDS and TOC rejection during filtration by the UF, NF90, and BW30 membranes. As can be seen, for the tighter BW30 and NF90 membranes, higher TDS rejection was obtained at pH 7. The 1,000 ppm WLS inlet feed TDS was reduced to 60–63 ppm at pH 9, 30 ppm at pH 7, and to 96 ppm at pH 10 by both the BW30 and NF90 membranes. The precipitation of silica nanoparticles and also the co-precipitation of organic compounds by adsorption onto the surface of the silica nanoparticles at lower pH resulted in the formation of a closely packed cake layer, which increased the TDS rejection by almost five percent. For the UF membrane, pH reduction decreased the TDS rejection. This rejection was found to be irreversible when the pH was increased back to 10. This interesting result confirms that irreversible pore blocking occurred with the loose UF membrane at lower pH values. After UF treatment, permeate TDS was reduced to 580 ppm at pH 9, 690 ppm at pH 7, and 750 ppm at pH 10.

The effect of pH on TOC rejection was relatively insignificant, particularly for salt rejecting membranes. At pH 9, TOC rejection increased over time due to cake filtration effects, then decreased very slightly as the pH decreased to 7. Cake filtration at lower pH was predicted to increase the TOC rejection similar to TDS rejection. However, the slight increase in TOC rejection may have been due to the precipitation of very small MWCO hydrophilic DOM molecules which could pass through both the cake layer and the membrane. According to Fig. 5, both the NF90 and BW30 membranes were able to reject 90–93% of the DOM. This minor change in TOC rejection is attributed to the larger size of the DOM molecules compared to the  $\text{Na}^+$  and  $\text{Cl}^-$  monovalent ions making up the TDS. DOM/membrane interactions at higher pH and DOM/cake layer interactions at lower pH had the same effect on the removal of DOM. In the case of the UF membrane, the deposition of precipitated DOM on the walls of the membrane's pores made the pores

narrower which improved screening performance. It must be noted that pore constriction for the UF membrane was insufficient to cause increased salt rejection, due to the very small size of the salt ions. On the contrary, TDS rejection decreased drastically due to the lower electrostatic repulsion for the fouled membrane.

### 3.3. Evaluation of membranes for WLS inlet filtration applications

In order to select a suitable membrane for SAGD WLS inlet filtration applications, the trade-off relationship between energy consumption and product quality was considered. In pressure-driven membrane processes, energy consumption is directly related to the applied trans-membrane pressure. Hence, UF and loose NF membranes are less energy intensive than tight NF and RO membranes. The applied pressure for the UF and NF270 membranes was 207 and 276 kPa, respectively. Based on the results shown in Figs. 3 and 5, TOC and TDS rejection increased considerably from about 50 and 30% for UF to more than 70% for NF270 just by applying 68.9 kPa more pressure. Therefore, when very high quality water is not

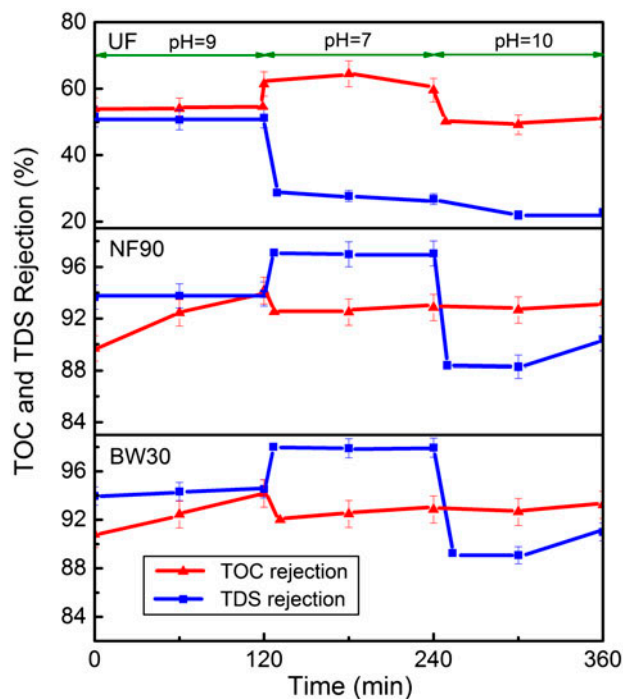


Fig. 5. TOC and TDS rejection during cross-flow filtration of WLS inlet water by UF, NF90, and BW30 membranes at various pH values (9–7–10). The transmembrane pressure was adjusted to 207, 552, and 827 kPa for UF, NF90 and BW30 membranes, respectively.

required, NF270 can be selected as an excellent energy efficient membrane.

The ESNA and NF90 membranes were found to give a 35 LMH water flux at the same trans-membrane pressure of 552 kPa. However, the TOC and TDS rejection of the NF90 membrane was slightly better than the ESNA membrane (Figs. 3 and 5). TDS rejection for the NF90 and the ESNA membranes were 93 and 91%, respectively. The initial TOC rejection for the NF90 membrane was also 4% higher than the ESNA membrane (90% compared to 86%). In fact, the water produced by the NF90 membrane had the same quality as that obtained with the RO BW30 and ESPA membranes, which operated at 827 kPa. Hence, the NF90 membrane is suggested as the best candidate, since it provided reasonable product quality and was found to be more energy efficient than the RO membrane.

### 3.4. Rejection of organic matter

DOM is a heterogeneous mixture of aromatic and aliphatic organic compounds containing oxygen, nitrogen, and sulfur functional groups (e.g. carboxyl, amine and thiol) [85]. Fluorescence excitation emission matrix spectroscopy (FEEMs) is a reliable and inexpensive method which can provide valuable information about the nature of the dissolved organics. This method has been used in our prior investigations of SAGD water characterization [4]. The FEEMs technique works by excitation of electrons to a higher energy level by absorption of light energy, and then by the release of energy as light as the excited electrons drop to a lower energy level. Aromatic organic compounds, like humic acids, which absorb and re-emit light, are called fluorophores. The excitation/emission (Ex/Em) wavelength ranges for peaks associated with pure organic compounds are obtained by researchers and can be used as scales to identify types of organic matter in a mixture. In our previous work, FEEM output was correlated to DOM classification by a resin-fractionation technique for this SAGD produced water stream [4].

Fig. 6 shows the FEEMs results for the DOM in the WLS inlet feedwater and the membrane permeates at pH 9. The fluorescence response for the WLS inlet feed was observed over a wide range of wavelengths, with a dominant peak at the Ex/Em wavelength range of 220–350/350–450. This wide range of wavelengths demonstrates that various types of organic compounds exist in the WLS inlet feed. The fluorescence peaks of DOM are generally caused by the presence of high aromaticity as well as the presence of hydroxyl (mainly in carboxylic acid), and amine (mainly in PA

polymer and/or amino acid organic matter) groups in the organic fluorophores. The fluorescence intensity of any fluorophore can be reduced by the interfering effects of other molecules present in a mixture of fluorophores.

According to Fig. 6, the WLS feed water used in this study contains a wide range of organic matter including hydrophilic acids (HPiA), hydrophilic bases (HPiB), hydrophilic neutrals (HPiN), hydrophobic acids (HPoA), hydrophobic bases (HPoB), and hydrophobic neutrals (HPoN), based on the classified results of our previous studies. This variety still exists in the permeate streams of the NF270 and UF membranes. This indicates that UF and looser NF membranes do not completely remove any of the organic matter types; all types of organics passed through the membranes to some extent. In the case of RO and tight NF membranes, the main organics in the permeate stream were hydrophilic compounds (HPiN, HPiA, and HPiB). This means that hydrophobic acids in the WLS inlet water, like humic acid, were almost completely removed by these membranes. Since the TOC rejection for NF and RO membranes increased with time (Figs. 3 and 5), it is concluded that the hydrophilic matter detected by the FEEMs technique was mainly passed through the membranes at the early stage of filtration. At the initial stage of filtration, the hydrophilic parts of the DOM in the WLS inlet water were in direct contact with the surface of the hydrophilic membranes. This facilitated their transfer to the permeate side. Hydrophobic organics are thought to be the main subgroup responsible for membrane fouling [27,28,81,86]. FEEMs results confirm that the hydrophobic subgroups of the organic matter in the WLS inlet water were mostly deposited on the membrane surface and made the fouling more severe, especially at the second stage of filtration when the hydrophobic interaction of organic matter becomes important. Fig. 6 suggests that tight NF and RO membranes are the most favorable membrane options for removing DOM from WLS inlet water.

### 3.5. Rejection of inorganics

Inductively coupled plasma-optical emission spectroscopy (ICP-OES) analysis was performed on the permeates of the UF, NF90, and BW30 membranes to determine the rejection of inorganic constituents in the WLS inlet water. The results are presented in Table 4. The total inorganic rejection for the NF90 and BW30 membranes was greater than 90%, which confirms our previous results on TDS rejection. The NF90 and BW30 membranes removed almost all of the divalent

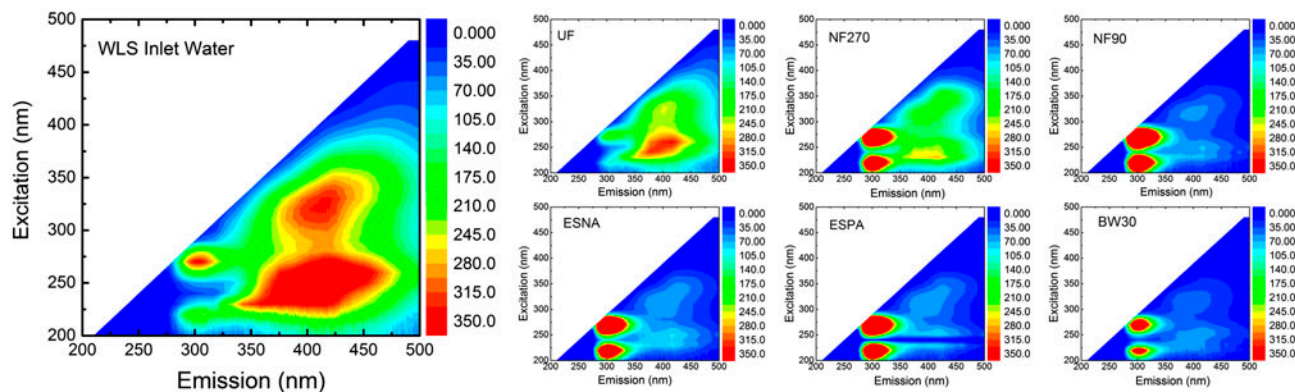


Fig. 6. Excitation–emission matrices (EEMs) of WLS inlet water and permeates at pH 9. Excitation at 5 nm intervals from 200 to 500 nm and emission data collected at an interval of 10 nm. All permeate samples and WLS inlet feed were diluted using DI water to a TOC level of  $15 \pm 5$  mg/L to avoid inner filtration (quenching) effects on fluorescence analysis. Dilution time was 10:1 for UF permeate, 5:1 for NF270 permeate, 2:1 for NF90, ESNA, ESPA, BW30 permeates and 20:1 for WLS inlet water. The color scale representing the fluorescence intensity is logarithmic in all parts of these images.

ions and iron in the feed. However, about 4% of the silica passed through these membranes. Sodium and chloride rejection by the NF90 and BW30 membranes was found to be essentially the same, at about 93 and 97%, respectively. The UF membrane rejected approximately 30, 20, and 75% of the silica, sodium, and calcium, respectively. This shows that the UF membrane was inefficient for the removal of inorganic materials and cannot be applied for WLS inlet water treatment. The low levels of inorganic, scale-forming species in the NF and RO permeate would greatly reduce the fouling propensity of the resulting BFW if NF and RO were applied as a polishing step in the conventional SAGD process train. According to the data presented in Table 4, it can be concluded that the NF90 membrane is the most promising alternative for removing inorganic material from WLS inlet water, considering both membrane performance and energy consumption.

### 3.6. Results of surface analyses

Fouled membranes were characterized by FESEM–EDX and ATR-FTIR to determine the elements deposited on the membrane surface. Furthermore, analysis of the fouled membranes was used to determine the fouling intensity at different pH values. The precipitation of more foulants on the membrane surface at lower pH and the re-dissolving of these deposits when the pH was increased can be clearly observed in the FESEM images.

#### 3.6.1. Field emission scanning electron microscope–energy dispersive X-ray (FESEM–EDX)

The morphology of the materials deposited on the membrane surface was qualitatively determined by FESEM analysis. Fig. 7 shows FESEM images of fouled membranes with a magnification of 5,000. As can be seen, more organic and inorganic materials were

Table 4  
Inorganic rejection for UF, NF90 and BW30 membranes

Elements	Unit	RDL <sup>a</sup>	Feed water	UF permeate	NF90 permeate	BW30 permeate
Boron (B)	mg/L	0.2	19 <sup>b</sup>	17 <sup>b</sup>	8.6 <sup>b</sup>	5.8 <sup>b</sup>
Calcium (Ca <sup>2+</sup> )	mg/L	0.3	1.9	0.42	<0.30	<0.30
Iron (total)	mg/L	0.06	0.39	<0.06	<0.06	<0.06
Magnesium (Mg <sup>2+</sup> )	mg/L	0.2	0.59	<0.20	<0.20	<0.20
Silica (dissolved silicon)	mg/L	0.1	89	61	2.9	3.2
Sodium (Na <sup>+</sup> )	mg/L	0.5	350	290	26	20
Chloride (Cl <sup>1-</sup> )	mg/L	1.0	170	120	5.3	3.8

<sup>a</sup>Reportable detection limit.

<sup>b</sup>Detection limits raised due to dilution to bring analyte within the calibrated range.

deposited on the membranes at lower pH values. In the case of the NF90 and BW30 membranes, increasing the pH back to 10 re-dissolved the deposited foulants. For these membranes, the surface of the membranes is not fully covered by the foulants, and the morphology of the virgin membrane is noticeable. This confirms the substantial effect of pH on flux recovery in salt rejecting NF and RO membranes.

The NF270, ESNA, and ESPA membranes were found to foul to a similar extent, although the morphologies of the fouled materials were found to be different. It must be noted that these  $20 \times 20 \mu\text{m}$  FESEM images are not representative of the whole effective membrane surface area ( $140 \text{ cm}^2$ ). For instance, the NF270 membrane is mostly covered by a black material which is assumed to be mainly pure organic

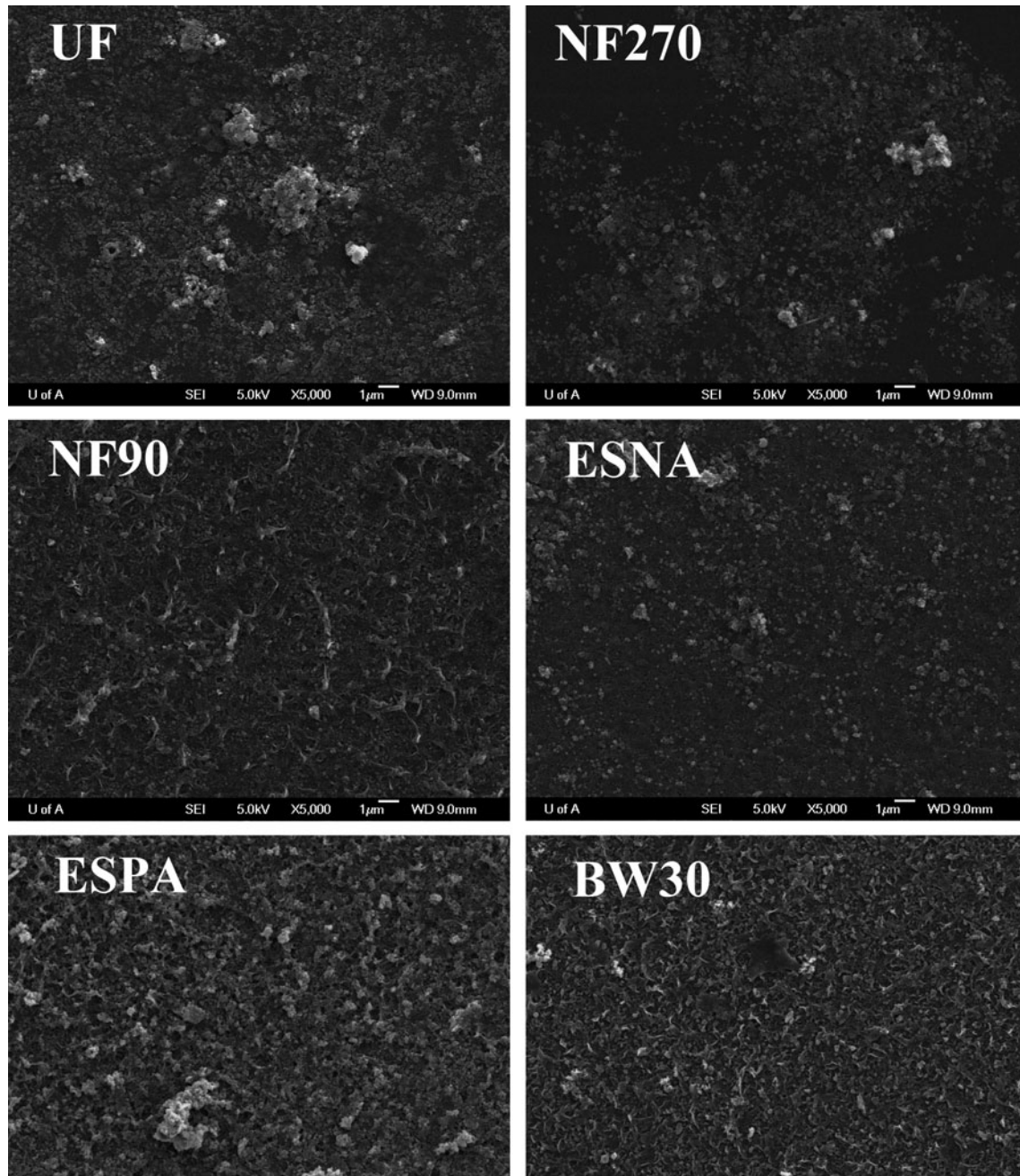


Fig. 7. FESEM image of fouled membranes by WLS inlet water at 5 k magnification.

matter. In the case of the ESNA and ESPA membranes, a mixture of organic and inorganic materials was deposited on the membrane, which is identifiable by the spongy structure of the cake layer.

The morphologies of the materials adsorbed on the membrane surface are more noticeable in the higher magnification images shown in Fig. 8. As can be seen, the deposited mass on the membrane is mainly in the form of particles which were determined by EDX analysis to be silica particles. The crystal shapes on the membrane surface were found to be iron and calcium crystals. The sponge-like shapes were found to contain sulfur, organic matter, and silica. Silica in the sponge-like shapes confirms co-precipitation of silica and organic matter on the membranes, especially at lower pH values. The size of these particles is about 100 nm—larger than expected—which demonstrates that the adsorption of organic matter occurs on the surface of silica particles.

### 3.6.2. ATR-FTIR results

All membrane samples were scanned with wavelengths of 500–4,000  $\text{cm}^{-1}$  and the FTIR peaks of virgin and fouled membranes are shown in Fig. 9. This figure shows that the peak heights related to the fouled membrane are reduced after filtration. Membranes prepared by Filmtec (NF270, NF90, and BW30) and GE (UF) clearly show different peaks from those of the Hydranautics membranes (ESNA and ESPA). This shows that the type of PA thin film in these membranes is different. All of these membranes show ATR-FTIR spectra peaks between 600 and 1,500  $\text{cm}^{-1}$ , which indicate the presence of the polysulfone inter-layer. Peaks at 1,650 and 1,541  $\text{cm}^{-1}$  indicate amide I and amide II for all membranes. All Filmtec membranes are made from m-phenylene diamine, a primary amine. Though WLS inlet filtration leads to a decrease in polyamide and polysulfone associated peak heights, no new peaks were detected. The

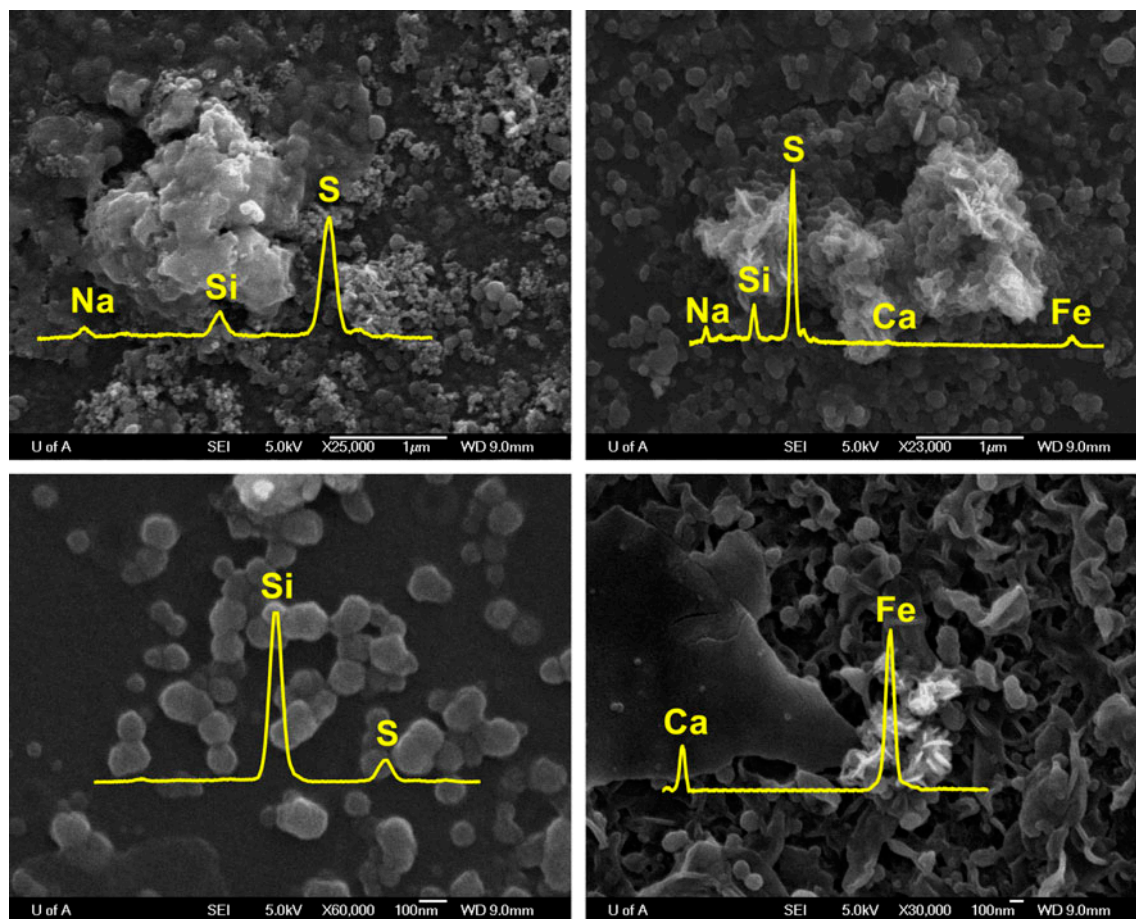


Fig. 8. Different morphologies of foulants observed by FESEM with corresponding EDX results.

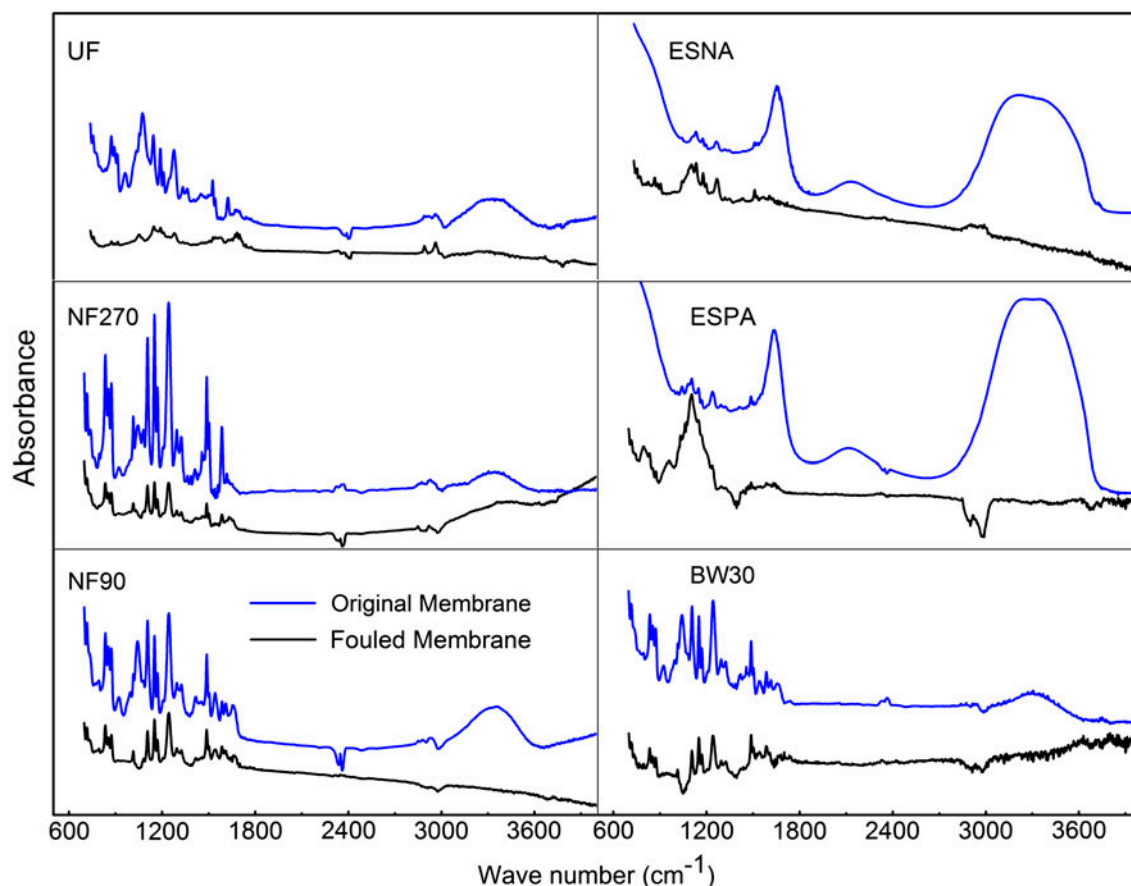


Fig. 9. ATR-FTIR spectra of applied membranes before and after WLS inlet filtration.

absence of peaks representing organic foulants is most likely due to the fact that the peaks associated with polysulfone and polyamide swamp any small peaks that represent adsorbed organic species.

#### 4. Conclusion

WLS inlet water from a SAGD process was treated with cross-flow UF, NF, and RO membranes at bench-scale. All experiments were conducted at a constant feed temperature (50°C) and various pH values. It was found that the more hydrophilic membranes with more negative surface charge and less roughness were less prone to fouling. RO and tight NF membranes removed more than 86% of the TDS and TOC. TOC rejection increased significantly over time due to clogging of hot spots by DOM and silica. Ultrafiltration was found to be unsuitable for SAGD produced water treatment due to its low performance in rejecting silica and DOM. However, a loose NF membrane was found to be a reasonable choice when very high purification of water is not necessary. The loose NF membrane

removed more than 70% of the TDS and TOC. Tight nanofiltration membranes (NF90 and ESNA) were found to produce high quality permeate comparable to RO while consuming less energy than RO. Flux, TOC rejection, and TDS rejection were found to be strongly affected by changes in solution pH. Acidification of WLS inlet water during operation (rapid pH change from 9 to 7) decreased the flux suddenly and increased the TDS rejection for tight NF and RO membranes. However, TOC rejection decreased slightly by decreasing the feed pH. The ultrafiltration membrane showed the exact opposite behavior due to the different fouling mechanism governing the transport of salt and DOM in loose membranes. Rapidly increasing the pH from 7.0 to 10.0 increased the water flux by about 40% immediately, which demonstrated the critical role of pH on fouling reduction. The re-dissolving of fouling deposits by increasing pH was observed from surface characterization data of the fouled membranes obtained with FESEM–EDX. ATR-FTIR and FESEM–EDX techniques provided valuable information about the constituents in the WLS inlet water which were

deposited on the membrane. EDX analysis indicated the presence of silica, iron and calcium in the fouling deposits. Fluorescence excitation emission matrix spectroscopy (FEEMs) showed that the major organic groups that passed through the membrane were hydrophilic compounds.

This study shows the feasibility of performing membrane processes at a high pH on WLS inlet water. The results can be interpreted to provide a possible process configuration for SAGD PW treatment. NF process can be seen as an alternative to the current WLS-IX process configuration, completely replacing the conventional treatment process, and providing reliable removal of TDS, silica, divalent ions, and TOC from the produced water.

### Acknowledgments

Financial support for this work through the NSERC Industrial Research Chair in Water Quality Management for Oil Sands Extraction is gratefully acknowledged. The authors would like to thank Dr Fleck (Professor, Chair of Mechanical Engineering Department, University of Alberta) for kindly supporting these water treatment projects and his helpful suggestions.

### References

- [1] R. Hill, Thermal in situ Water Conservation Study, Technical Report, AI-EES and Jacobs Consultancy, Edmonton, 2012.
- [2] D.W. Jennings, A. Shaikh, Heat-exchanger deposition in an inverted steam-assisted gravity drainage operation. Part 1. Inorganic and organic analyses of deposit samples, *Energy Fuels* 21 (2007) 176–184.
- [3] S. Wang, E. Axcell, R. Bosch, V. Little, Effects of chemical application on antifouling in steam-assisted gravity drainage operations, *Energy Fuels* 19 (2005) 1425–1429, doi: [10.1021/ef0498081](https://doi.org/10.1021/ef0498081).
- [4] S. Guha Thakurta, A. Maiti, D.J. Pernitsky, S. Bhattacharjee, Dissolved organic matter in steam assisted gravity drainage boiler blow-down water, *Energy Fuels* 27 (2013) 3883–3890, doi: [10.1021/ef4002154](https://doi.org/10.1021/ef4002154).
- [5] W.F. Heins, Is a paradigm shift in produced water treatment technology occurring at SAGD facilities? *J. Can. Pet. Technol.* 49 (2010) 10–15.
- [6] W.F. Heins, Technical advancements in SAGD evaporative produced water treatment, *J. Can. Pet. Technol.* 48 (2009) 27–32.
- [7] E.W. Allen, Process water treatment in Canada's oil sands industry: II. A review of emerging technologies, *J. Environ. Eng. Sci.* 7 (2008) 499–524, doi: [10.1139/S08-020](https://doi.org/10.1139/S08-020).
- [8] T. Bilstad, E. Espedal, Membrane separation of produced water, *Water Res.* 34 (1996) 239–246.
- [9] J.C. Campos, R.M.H. Borges, A.M. Oliveira Filho, R. Nobrega, G.L. Sant'Anna Jr., J. Sant'Anna, Oilfield wastewater treatment by combined microfiltration and biological processes, *Water Res.* 36 (2002) 95–104. Available from: <http://www.ncbi.nlm.nih.gov/pubmed/11767743>.
- [10] J. Zhong, X. Sun, C. Wang, Treatment of oily wastewater produced from refinery processes using flocculation and ceramic membrane filtration, *Sep. Purif. Technol.* 32 (2003) 93–98.
- [11] A.I. Schäfer, Natural Organics Removal using Membranes, The University of New South Wales, Sydney, 1999.
- [12] S.M. Santos, M.R. Wiesner, Ultrafiltration of water generated in oil and gas production, *Water Environ. Res.* 69 (1997) 1120–1127.
- [13] E.-S.S. Kim, Y. Liu, M. Gamal El-Din, The effects of pretreatment on nanofiltration and reverse osmosis membrane filtration for desalination of oil sands process-affected water, *Sep. Purif. Technol.* 81 (2011) 418–428, doi: [10.1016/j.seppur.2011.08.016](https://doi.org/10.1016/j.seppur.2011.08.016).
- [14] H. Peng, K. Volchek, M. MacKinnon, W.P. Wong, C.E. Brown, Application of nanofiltration to water management options for oil sands operation, *Desalination* 170 (2004) 137–150, doi: [10.1016/j.desal.2004.03.018](https://doi.org/10.1016/j.desal.2004.03.018).
- [15] A.B.A.K. Mehrotra, Evaluation of reverse osmosis for the treatment of oil sands produced water, *Water Pollut. Res. J. Can.* 21 (1986) 141–152.
- [16] M. Sadrzadeh, J. Hajinasiri, S. Bhattacharjee, D. Pernitsky, Nanofiltration of oil sands boiler feed water: Effect of pH on water flux and organic and dissolved solid rejection, *Sep. Purif. Technol.* 141 (2015) 339–353, doi: [10.1016/j.seppur.2014.12.011](https://doi.org/10.1016/j.seppur.2014.12.011).
- [17] S. Hong, M. Elimelech, Chemical and physical aspects of natural organic matter (NOM) fouling of nanofiltration membranes, *J. Membr. Sci.* 132 (1997) 159–181, doi: [10.1016/S0376-7388\(97\)00060-4](https://doi.org/10.1016/S0376-7388(97)00060-4).
- [18] M. Gamal El-Din, H. Fu, N. Wang, P. Chelme-Ayala, L. Pérez-Estrada, P. Drzewicz, Naphthenic acids speciation and removal during petroleum-coke adsorption and ozonation of oil sands process-affected water, *Sci. Total Environ.* 409 (2011) 5119–5125, doi: [10.1016/j.scitotenv.2011.08.033](https://doi.org/10.1016/j.scitotenv.2011.08.033).
- [19] A.C. Scott, W. Zubot, M.D. MacKinnon, D.W. Smith, P.M. Fedorak, Ozonation of oil sands process water removes naphthenic acids and toxicity, *Chemosphere* 71 (2008) 156–160, doi: [10.1016/j.chemosphere.2007.10.051](https://doi.org/10.1016/j.chemosphere.2007.10.051).
- [20] E. Quagraine, H. Peterson, J. Headley, In situ bioremediation of naphthenic acids contaminated tailing pond waters in the Athabasca oil sands region—Demonstrated field studies and plausible options: A review, *J. Environ. Sci. Health Part A Toxic/Hazard. Subst. Environ. Eng.* 40 (2005) 685–722, doi: [10.1081/ESE-200046649](https://doi.org/10.1081/ESE-200046649).
- [21] M.D. MacKinnon, H. Boerger, Description of two treatment methods for detoxifying oil sands tailings pond water, *Water Pollut. Res. J. Can.* 21 (1986) 496–512.
- [22] J.S. Clemente, P.M. Fedorak, A review of the occurrence, analyses, toxicity, and biodegradation of naphthenic acids, *Chemosphere* 60 (2005) 585–600, doi: [10.1016/j.chemosphere.2005.02.065](https://doi.org/10.1016/j.chemosphere.2005.02.065).
- [23] H. Kawaguchi, Z. Li, Y. Masuda, K. Sato, H. Nakagawa, Dissolved organic compounds in reused process water for steam-assisted gravity

- drainage oil sands extraction, *Water Res.* 46 (2012) 5566–5574, doi: [10.1016/j.watres.2012.07.036](https://doi.org/10.1016/j.watres.2012.07.036).
- [24] M.A. Petersen, H. Grade, Analysis of steam assisted gravity drainage produced water using two-dimensional gas chromatography with time-of-flight mass spectrometry, *Ind. Eng. Chem. Res.* 50 (2011) 12217–12224, doi: [10.1021/ie200531h](https://doi.org/10.1021/ie200531h).
- [25] Q. Li, M. Elimelech, organic fouling and chemical cleaning of nanofiltration membranes: measurements and mechanisms, *Environ. Sci. Technol.* 38 (2004) 4683–4693. Available from: <http://www.ncbi.nlm.nih.gov/pubmed/15461180>.
- [26] C. Bellona, M. Marts, J.E. Drewes, The effect of organic membrane fouling on the properties and rejection characteristics of nanofiltration membranes, *Sep. Purif. Technol.* 74 (2010) 44–54, doi: [10.1016/j.seppur.2010.05.006](https://doi.org/10.1016/j.seppur.2010.05.006).
- [27] Anne Braghetta, F.A. DiGiano, W.P. Ball, NOM accumulation at NF membrane surface: Impact of chemistry and shear, *J. Environ. Eng.* 124 (1998) 1087–1098.
- [28] C. Jucker, M.M. Clark, Adsorption of aquatic humic substances on hydrophobic ultrafiltration membranes, *J. Membr. Sci.* 97 (1994) 37–52.
- [29] S. Mondal, S.R. Wickramasinghe, Produced water treatment by nanofiltration and reverse osmosis membranes, *J. Membr. Sci.* 322 (2008) 162–170, doi: [10.1016/j.memsci.2008.05.039](https://doi.org/10.1016/j.memsci.2008.05.039).
- [30] D.A. Patterson, L. Yen Lau, C. Roengpithya, E.J. Gibbins, A.G. Livingston, Membrane selectivity in the organic solvent nanofiltration of trialkylamine bases, *Desalination* 218 (2008) 248–256, doi: [10.1016/j.desal.2007.02.020](https://doi.org/10.1016/j.desal.2007.02.020).
- [31] H. Dach, Comparison des opérations de nanofiltration et d'osmose inverse pour le dessalement sélectif des eaux saumâtres: De l'échelle du laboratoire au pilote industriel (Comparison of nanofiltration and reverse osmosis processes for a selective desalination of brackish water feeds), University of Angers, Angers, 2008.
- [32] M.J. López-Muñoz, A. Sotto, J.M. Arsuaga, B. Van der Bruggen, Influence of membrane, solute and solution properties on the retention of phenolic compounds in aqueous solution by nanofiltration membranes, *Sep. Purif. Technol.* 66 (2009) 194–201, doi: [10.1016/j.seppur.2008.11.001](https://doi.org/10.1016/j.seppur.2008.11.001).
- [33] A.R.S. Teixeira, J.L.C. Santos, J.G. Crespo, Sustainable membrane-based process for valorisation of cork boiling wastewaters, *Sep. Purif. Technol.* 66 (2009) 35–44, doi: [10.1016/j.seppur.2008.12.001](https://doi.org/10.1016/j.seppur.2008.12.001).
- [34] A. Alturki, N. Tadkaew, J. McDonald, S.J. Khan, W.E. Price, L.D. Nghiem, Combining MBR and NF/RO membrane filtration for the removal of trace organics in indirect potable water reuse applications, *J. Membr. Sci.* 365 (2010) 206–215, doi: [10.1016/j.memsci.2010.09.008](https://doi.org/10.1016/j.memsci.2010.09.008).
- [35] D. Nanda, K.-L. Tung, C.-C. Hsiung, C.-J. Chuang, R.-C. Ruaan, Y.-C. Chiang, C.-S. Chen, T.-H. Wu, Effect of solution chemistry on water softening using charged nanofiltration membranes, *Desalination* 234 (2008) 344–353, doi: [10.1016/j.desal.2007.09.103](https://doi.org/10.1016/j.desal.2007.09.103).
- [36] K. Kimura, G. Amy, J.E. Drewes, T. Heberer, T.U. Kim, Y. Watanabe, Rejection of organic micropollutants (disinfection by-products, endocrine disrupting compounds, and pharmaceutically active compounds) by NF/RO membranes, *J. Membr. Sci.* 227 (2003) 113–121, doi: [10.1016/j.memsci.2003.09.005](https://doi.org/10.1016/j.memsci.2003.09.005).
- [37] W. Peng, I. Escobar, D. White, Effects of water chemistries and properties of membrane on the performance and fouling—A model development study, *J. Membr. Sci.* 238 (2004) 33–46, doi: [10.1016/j.memsci.2004.02.035](https://doi.org/10.1016/j.memsci.2004.02.035).
- [38] K.L. Tu, A.R. Chivas, L.D. Nghiem, Effects of membrane fouling and scaling on boron rejection by nanofiltration and reverse osmosis membranes, *Desalination* 279 (2011) 269–277, doi: [10.1016/j.desal.2011.06.019](https://doi.org/10.1016/j.desal.2011.06.019).
- [39] J.J. Lee, Removal of Microcystin-LR from Drinking Water using Adsorption and Membrane Processes, PhD Thesis, The Ohio State University, Columbus, 2009.
- [40] Y. Wang, C.Y. Tang, Protein fouling of nanofiltration, reverse osmosis, and ultrafiltration membranes—The role of hydrodynamic conditions, solution chemistry, and membrane properties, *J. Membr. Sci.* 376 (2011) 275–282, doi: [10.1016/j.memsci.2011.04.036](https://doi.org/10.1016/j.memsci.2011.04.036).
- [41] Y. Yoon, P. Westerhoff, J. Yoon, S.A. Snyder, Removal of 17 $\beta$  estradiol and fluoranthene by nanofiltration and ultrafiltration, *J. Environ. Eng.* 130 (2004) 1460–1467, doi: [10.1061/\(ASCE\)0733-9372\(2004\)130:12\(1460\)](https://doi.org/10.1061/(ASCE)0733-9372(2004)130:12(1460)).
- [42] R. Bernstein, S. Belfer, V. Freger, Bacterial attachment to RO membranes surface-modified by concentration-polarization-enhanced graft polymerization, *Environ. Sci. Technol.* 45 (2011) 5973–5980, doi: [10.1021/es1043694](https://doi.org/10.1021/es1043694).
- [43] F. Fadhillah, S.M.J. Zaidi, Z. Khan, M.M. Khaled, F. Rahman, P.T. Hammond, Development of polyelectrolyte multilayer thin film composite membrane for water desalination application, *Desalination* 318 (2013) 19–24, doi: [10.1016/j.desal.2013.03.011](https://doi.org/10.1016/j.desal.2013.03.011).
- [44] L.D. Nghiem, S. Hawkes, Effects of membrane fouling on the nanofiltration of pharmaceutically active compounds (PhACs): Mechanisms and role of membrane pore size, *Sep. Purif. Technol.* 57 (2007) 176–184.
- [45] P. Xu, J. Drewes, T.U. Kim, C. Bellona, G. Amy, Effect of membrane fouling on transport of organic contaminants in NF/RO membrane applications, *J. Membr. Sci.* 279 (2006) 165–175, doi: [10.1016/j.memsci.2005.12.001](https://doi.org/10.1016/j.memsci.2005.12.001).
- [46] K.P. Ishida, R. Bold, D.W. Phipps Jr., Identification and Evaluation of Unique Chemicals for Optimum Membrane Compatibility and Improved Cleaning Efficiency, Final Report, Orange County Water District and California Department of Water Resources, Fountain Valley, CA, 2005.
- [47] M. Hesampour, J. Tanninen, S. Reinikainen, S. Platt, M. Nyström, Nanofiltration of single and mixed salt solutions: Analysis of results using principal component analysis (PCA), *Chem. Eng. Res. Des.* 88 (2010) 1569–1579.
- [48] J. Tanninen, M. Mänttari, M. Nyström, Effect of salt mixture concentration on fractionation with NF membranes, *J. Membr. Sci.* 283 (2006) 57–64.
- [49] A.J.C. Semião, A.I. Schäfer, Removal of adsorbing estrogenic micropollutants by nanofiltration membranes. Part A—Experimental evidence, *J. Membr. Sci.* 431 (2013) 244–256, doi: [10.1016/j.memsci.2012.11.080](https://doi.org/10.1016/j.memsci.2012.11.080).
- [50] C. Bellona, J.E. Drewes, The role of membrane surface charge and solute physico-chemical properties in the rejection of organic acids by NF membranes, *J. Membr. Sci.* 249 (2005) 227–234, doi: [10.1016/j.memsci.2004.09.041](https://doi.org/10.1016/j.memsci.2004.09.041).

- [51] O.C. Nieto, Quantitative Characterization of Physico-Chemical Properties of the Active Layers of Reverse Osmosis and Nanofiltration Membranes, and their Relation to Membrane Performance, PhD Thesis, University of Illinois at Urbana-Champaign, Champaign, 2010.
- [52] L. Llenas, X. Martínez-Lladó, A. Yaroshchuk, M. Rovira, J. de Pablo, Nanofiltration as pretreatment for scale prevention in seawater reverse osmosis desalination, *Desalin. Water Treat.* 36 (2011) 310–318, doi: [10.5004/dwt.2011.2767](https://doi.org/10.5004/dwt.2011.2767).
- [53] E.M. Vrijenhoek, S. Hong, M. Elimelech, Influence of membrane surface properties on initial rate of colloidal fouling of reverse osmosis and nanofiltration membranes, *J. Membr. Sci.* 188 (2001) 115–128.
- [54] R.J. Wakeman, C.J. Williams, Additional techniques to improve microfiltration, *Sep. Purif. Technol.* 26 (2002) 3–18, doi: [10.1016/S1383-5866\(01\)00112-5](https://doi.org/10.1016/S1383-5866(01)00112-5).
- [55] O. Gundogdu, M.A. Koenders, R.J. Wakeman, P. Wu, Permeation through a bed on a vibrating medium: Theory and experimental results, *Chem. Eng. Sci.* 58 (2003) 1703–1713, doi: [10.1016/S0009-2509\(03\)00019-8](https://doi.org/10.1016/S0009-2509(03)00019-8).
- [56] S. Muthukumar, S. Kentish, M. Ashokkumar, G. Stevens, Mechanisms for the ultrasonic enhancement of dairy whey ultrafiltration, *J. Membr. Sci.* 258 (2005) 106–114, doi: [10.1016/j.memsci.2005.03.001](https://doi.org/10.1016/j.memsci.2005.03.001).
- [57] M.R. Guilherme, G.M. Campese, E. Radovanovic, A.F. Rubira, E.B. Tambourgi, E.C. Muniz, Thermo-responsive sandwiched-like membranes of IPN-PNIPAAm/PAAm hydrogels, *J. Membr. Sci.* 275 (2006) 187–194.
- [58] R.P. Shaikh, V. Pillay, Y.E. Choonara, L.C. du Toit, V.M.K. Ndesendo, P. Bawa, S. Cooppan, A review of multi-responsive membranous systems for rate-modulated drug delivery, *AAPS PharmSciTech.* 11 (2010) 441–459, doi: [10.1208/s12249-010-9403-2](https://doi.org/10.1208/s12249-010-9403-2).
- [59] D. Wandera, S.R. Wickramasinghe, S.M. Husson, Stimuli-responsive membranes, *J. Membr. Sci.* 357 (2010) 6–35, doi: [10.1016/j.memsci.2010.03.046](https://doi.org/10.1016/j.memsci.2010.03.046).
- [60] C.Y. Tang, Y.-N. Kwon, J.O. Leckie, Fouling of reverse osmosis and nanofiltration membranes by humic acid—Effects of solution composition and hydrodynamic conditions, *J. Membr. Sci.* 290 (2007) 86–94, doi: [10.1016/j.memsci.2006.12.017](https://doi.org/10.1016/j.memsci.2006.12.017).
- [61] C.Y. Tang, Y.-N. Kwon, J.O. Leckie, Characterization of humic acid fouled reverse osmosis and nanofiltration membranes by transmission electron microscopy and streaming potential measurements, *Environ. Sci. Technol.* 41 (2007) 942–949. Available from: <http://www.ncbi.nlm.nih.gov/pubmed/17328207>.
- [62] Y.-N. Wang, C.Y. Tang, Nanofiltration membrane fouling by oppositely charged macromolecules: Investigation on flux behavior, foulant mass deposition, and solute rejection, *Environ. Sci. Technol.* 45 (2011) 8941–8947, doi: [10.1021/es202709r](https://doi.org/10.1021/es202709r).
- [63] J. Cho, G. Amy, J. Pellegrino, Membrane filtration of natural organic matter: Comparison of flux decline, NOM rejection, and foulants during filtration with three UF membranes, *Desalination* 127 (2000) 283–298, doi: [10.1016/S0011-9164\(00\)00017-5](https://doi.org/10.1016/S0011-9164(00)00017-5).
- [64] A.E. Childress, M. Elimelech, Effect of solution chemistry on the surface charge of polymeric reverse osmosis and nanofiltration membranes, *J. Membr. Sci.* 119 (1996) 253–268.
- [65] M. Elimelech, X. Xiaohua Zhu, A.E. Childress, S. Seungkwan Hong, Role of membrane surface morphology in colloidal fouling of cellulose acetate and composite aromatic polyamide reverse osmosis membranes, *J. Membr. Sci.* 127 (1997) 101–109.
- [66] E.M.V. Hoek, A.S. Kim, M. Elimelech, Influence of crossflow membrane filter geometry and shear rate on colloidal fouling in reverse osmosis and nanofiltration separations, *Environ. Eng. Sci.* 19 (2002) 357–372, doi: [10.1089/109287502320963364](https://doi.org/10.1089/109287502320963364).
- [67] Q. Li, Z. Xu, I. Pinnau, Fouling of reverse osmosis membranes by biopolymers in wastewater secondary effluent: Role of membrane surface properties and initial permeate flux, *J. Membr. Sci.* 290 (2007) 173–181.
- [68] L.D. Nghiem, S. Hawkes, Effects of membrane fouling on the nanofiltration of trace organic contaminants, *Desalination* 236 (2009) 273–281, doi: [10.1016/j.desal.2007.10.077](https://doi.org/10.1016/j.desal.2007.10.077).
- [69] S. Lee, M. Elimelech, Relating organic fouling of reverse osmosis membranes to intermolecular adhesion forces, *Environ. Sci. Technol.* 40 (2006) 980–987. Available from: <http://www.ncbi.nlm.nih.gov/pubmed/16509346>.
- [70] L.D. Nghiem, P.J. Coleman, NF/RO filtration of the hydrophobic ionogenic compound triclosan: Transport mechanisms and the influence of membrane fouling, *Sep. Purif. Technol.* 62 (2008) 709–716, doi: [10.1016/j.seppur.2008.03.027](https://doi.org/10.1016/j.seppur.2008.03.027).
- [71] W.E.I. Yuan, A.L. Zydney, Humic acid fouling during ultrafiltration, *Environ. Sci. Technol.* 34 (2000) 5043–5050.
- [72] C. Combe, E. Molis, P. Lucas, R. Riley, M.M. Clark, The effect of CA membrane properties on adsorptive fouling by humic acid, *J. Membr. Sci.* 154 (1999) 73–87, doi: [10.1016/S0376-7388\(98\)00268-3](https://doi.org/10.1016/S0376-7388(98)00268-3).
- [73] E.M.V. Hoek, M. Elimelech, Cake-enhanced concentration polarization: A new fouling mechanism for salt-rejecting membranes, *Environ. Sci. Technol.* 37 (2003) 5581–5588, doi: [10.1021/es0262636](https://doi.org/10.1021/es0262636).
- [74] S. Lee, J. Cho, M. Elimelech, Influence of colloidal fouling and feed water recovery on salt rejection of RO and NF membranes, *Desalination* 160 (2004) 1–12.
- [75] A. Maiti, M. Sadrezadeh, S. Guha Thakurta, D.J. Pernitsky, S. Bhattacharjee, M. Sadrzadeh, Characterization of boiler blowdown water from steam-assisted gravity drainage and silica-organic coprecipitation during acidification and ultrafiltration, *Energy Fuels* 26 (2012) 5604–5612, doi: [10.1021/ef300865e](https://doi.org/10.1021/ef300865e).
- [76] H. Guleryuz, I. Kaus, C. Filiàtre, T. Grande, M.-A. Einarsrud, Deposition of silica thin films formed by sol-gel method, *J. Sol-Gel Sci. Technol.* 54 (2010) 249–257, doi: [10.1007/s10971-010-2190-0](https://doi.org/10.1007/s10971-010-2190-0).
- [77] K. Rezwani, A.R. Studart, J. Vörös, L.J. Gauckler, Change of  $\zeta$  potential of biocompatible colloidal oxide particles upon adsorption of bovine serum albumin and lysozyme, *J. Phys. Chem. B.* 109 (2005) 14469–14474, doi: [10.1021/jp050528w](https://doi.org/10.1021/jp050528w).
- [78] W. Yuan, A.L. Zydney, Effects of solution environment on humic acid fouling during microfiltration, *Desalination* 122 (1999) 63–76, doi: [10.1016/S0011-9164\(99\)00028-4](https://doi.org/10.1016/S0011-9164(99)00028-4).
- [79] Z. Wang, Y. Zhao, J. Wang, S. Wang, Studies on nanofiltration membrane fouling in the treatment of water solutions containing humic acids, *Desalination* 178 (2005) 171–178, doi: [10.1016/j.desal.2004.11.036](https://doi.org/10.1016/j.desal.2004.11.036).
- [80] M. Kabsch-Korbutowicz, K. Majewska-Nowak, T. Winnicki, Analysis of membrane fouling in the treatment of water solutions containing humic acids and mineral salts, *Desalination* 126 (1999) 179–185, doi: [10.1016/S0011-9164\(99\)00172-1](https://doi.org/10.1016/S0011-9164(99)00172-1).

- [81] A. Braghetta, F.A. DiGiano, W.P. Ball, Nanofiltration of natural organic matter: pH and ionic strength effects, *J. Environ. Eng.* 123 (1997) 628–641.
- [82] K.L. Jones, C.R. O'Melia, Protein and humic acid adsorption onto hydrophilic membrane surfaces: Effects of pH and ionic strength, *J. Membr. Sci.* 165 (2000) 31–46, doi: [10.1016/S0376-7388\(99\)00218-5](https://doi.org/10.1016/S0376-7388(99)00218-5).
- [83] M.R. Teixeira, M.J. Rosa, pH adjustment for seasonal control of UF fouling by natural waters, *Desalination* 151 (2002) 165–175.
- [84] M. Elimelech, A.E. Childress, Zeta Potential of Reverse Osmosis Membranes: Implications for Membrane Performance, Final Report, UCLA University (Dr. Elimelech) and Denver Bureau of Reclamation, Los Angeles, CA, 1996.
- [85] W. Chen, P. Westerhoff, J.A. Leenheer, K. Booksh, Fluorescence excitation–emission matrix regional integration to quantify spectra for dissolved organic matter, *Environ. Sci. Technol.* 37 (2003) 5701–5710. Available from: <<http://www.ncbi.nlm.nih.gov/pubmed/14717183>>.
- [86] Y. Bessiere, B. Jefferson, E. Goslan, P. Bacchin, Effect of hydrophilic/hydrophobic fractions of natural organic matter on irreversible fouling of membranes, *Desalination* 249 (2009) 182–187, doi: [10.1016/j.desal.2008.12.047](https://doi.org/10.1016/j.desal.2008.12.047).